Prediction of Electrical Contact Resistance of Tin-Plated and Silver-Plated Terminals

Shigeru SAWADA*, Kaori SHIMIZU, Shigeki SHIMADA and Yasuhiro HATTORI

For virtual connector designing, it is important to predict contact resistance at a mating point. This study investigated the relationship between contact load and contact resistance in terms of contact shape, plating material and plating thickness. Tin plated and silver plated copper alloy samples were used. The contact resistance between an embossment pattern and a flat plate was measured by the four-probe method, and the indentation contact area was examined using an optical microscope. This study consisted of two phases: the analysis of load-contact area relationship by FEM (Finite Element Method), and that of contact area-resistance relationship based on the constriction resistance theory with plated layers. For a silver plated sample, which has no oxide films, the experimental results agreed with the theoretical prediction. Meanwhile, the results of a tin plated sample, which has oxide films, corresponded to the theoretical prediction at a high load region, in which terminal connectors are practically used. Thus it has become possible to predict a load-contact resistance curve.

Keywords: electrical contact, contact resistance, plating, contact load, contact area

1. Introduction

Automotive wiring harness helps the interaction between electrical equipment such as in-vehicle controllers, sensors, actuators, and lamps. An automotive connector, on the other hand, is one of the important parts, which connects wiring harness to other harnesses or electrical devices.

Automotive connector terminals are generally made of tin, gold and silver plated copper alloys. **Figure 1** shows an example of a sectional drawing of the terminals in engagement status. The female terminal has a spring made of copper alloy. An electric current can flow between the male and female terminals because these terminals have a mechanical contact caused by the force of the spring. For the design of new connectors, the terminal resistance must be known before starting the trial-production of the terminals. For this reason, it is important to predict electric contact resistance influenced by terminal design factor such as contact force, contact shape, plating material and plating thickness.
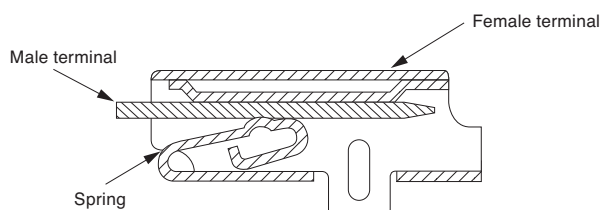

Fig. 1. Cross-section view of typical connector at mating situation

Many researchers have studied the relationship between contact load and contact resistance under various conditions[1]-[7]. F. Ossart et al. attempted the prediction of contact resistance in a 3N or lower-load region by the contact analysis using the Finite Element Method (FEM) [1]. X. Hernot et al. discussed the relationship between contact resistance and contact load on not-plated copper alloy contacts in a load range of up to 10N[4]. These researches are attempt to the region of less then 10N. Recently, the necessity of high-current terminals has become important for electric vehicles. Such terminals require sliver-plating as surface treatment, and require a high contact load as compared with conventional terminals. However, there are not any researches of predicting the contact resistance between plated terminals with a load exceeding 10N. Therefore the authors attempted the prediction of a contact-resistance load curve of tin-plated and silver-plated terminals in a high-load region.

2. Techniques for Prediction of Contact Resistance

Holm reported that the electric contact has the real contact area called as A-Spot in apparent contact area which produced by surface roughness or dirt. This contact image model is shown in **Fig.2**[5].
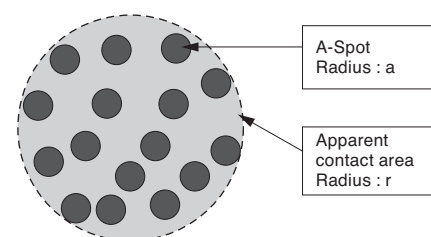

Fig. 2. Image of real contact points in apparent contact area

The contact resistance of A-Spot is represented as the sum of constriction resistance and film resistance by using the following **Equation (1)** reported by Holm[8]:

$$R_k = \frac{\rho}{2a} + \frac{\rho_f d}{\pi a^2} \qquad \cdots\cdots\cdots\cdots\cdots\cdots\cdots\cdots\cdots \quad (1)$$

where ρ indicates the resistivity of a contact material, a indicates a contact radius, ρ_f indicates the resistivity of a film, and d indicates the thickness of the film. It is reported that the constriction resistance is dominant in the load over 10N[6]. Therefore the constriction resistance is analyzed in this study.

Holm proposed the following approximation **Equation (2)** for constriction resistance in case of **Fig. 2**[9]:

$$R_k = \frac{\rho}{2r} + \frac{\rho}{2na} \qquad \cdots\cdots\cdots\cdots\cdots\cdots\cdots\cdots \quad (2)$$

where r indicates the radius of an apparent contact area, n indicates the number of A-spots, and a indicates the radius of A-Spot.

Greenwood released the following contact-resistance approximation **Equation (3)** for multiple contacts by considering the interaction between A-Spots[10].

$$R_k = \frac{\rho}{2\sum a_i} + \frac{\rho}{\pi} \left(\sum_{i \neq j}\sum \frac{a_i a_j}{S_{ij}} \right) \frac{1}{(\sum a_i)^2} \qquad \cdots\cdots\cdots\cdots\cdots \quad (3)$$

where S_{ij} indicates the distance between A-spots, and a_i, a_j indicates the radius of A-spot.

Figure 3 shows an example of contact resistance changing the radius of spots. The horizontal axis of **Fig. 3** indicates the rate of the real contact area in the apparent contact area. The vertical axis indicates the rate of the contact resistance compared with that the rate of real contact area is 1. When the rate of the real contact area is about 0.2, the rate of contact resistance increases only about 1.14-1.25 times. Therefore, in this research, it is assumed that the constriction resistance of apparent contact area is almost same as that of the real contact area presented by **Equation (4)**.
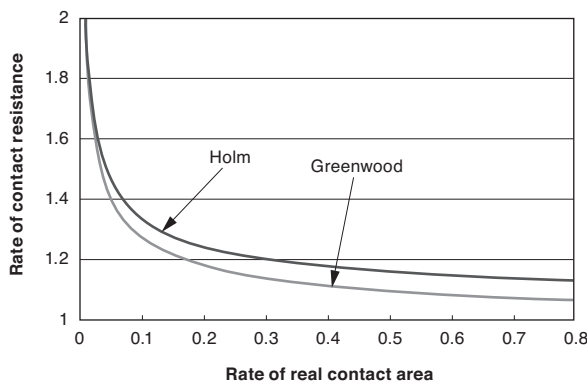
$$R_k = \frac{\rho}{2r} \qquad \cdots\cdots\cdots\cdots\cdots\cdots\cdots\cdots\cdots\cdots \quad (4)$$

The prediction of contact resistance is examined separately in two parts: mechanical contact which is related contact load with contact area, and electrical connection which is related contact area with contact resistance.

3. Experimental Method and Results

Specimens are commercial copper alloy for connectors with a layer of tin or silver plating, and also for non-plated samples prepared as a reference (see **Table 1**). The specimens have a hemispherical shape as an embossment with a radius 1-3 mm (see **Fig. 4**). The contact configuration in this study simulates contact of terminal mating. A schematic diagram of the apparatus to measure the contact resistance and load simultaneously is shown in **Fig. 5**[7]. The maximum

Table 1. Sample Conditions

Plating Material	Plating Thickness (μm)	Embossment Radius (mm)
Tin (matte)	1	1
	3	1
	5	1
Silver	2	3
	6	3
None	−	1, 3

Fig. 4. Sample shape

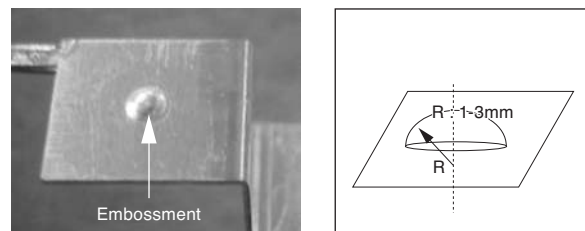Fig. 3. Relationship between rate of contact resistance and rate of real contact area in apparent contact area
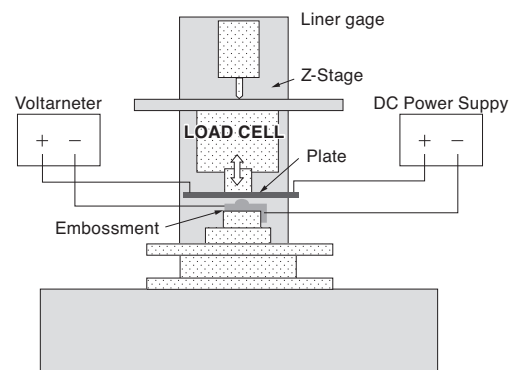

Fig. 5. Measurement Apparatus

contact load was chosen as 40N; the current was 1A, which is applied for a large current terminal. After measurement of the relationship between contact load and contact resistance, the contact traces were observed by an optical microscope and SEM (Scanning Electron Microscope). The apparent contact area is defined as the projected area of indentation measured by image software using the picture from the optical microscope. However, the contact area of non-plated samples could not be observed in resistance measurement samples. Therefore, other samples were used as a copper sulfureted layer coating, which is soft and thin in order to obtain the contact area.

The typical results of the relationship between contact resistance and contact load in the case of 6 µm silver plating and 5 µm tin plating are shown in **Fig. 6**. The contact resistance is lower at higher load, and the contact resistance of silver plating is lower than that of tin plating.

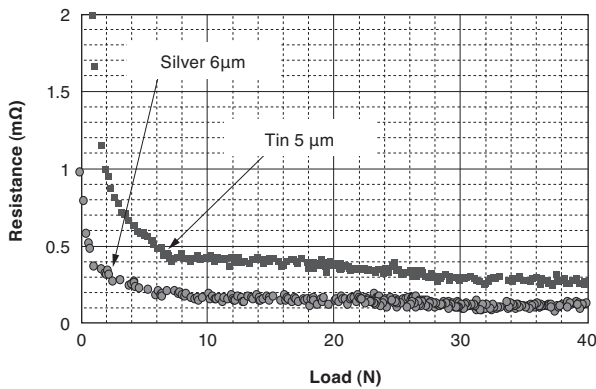**Fig. 8.** Typical results of the relationship between contact load and indentation contact area

Fig. 6. Typical example relationship between contact load and contact resistance for silver and tin plating

The typical SEM images and optical microscope image of the contact area under a condition of 1 µm tin plating and embossment radius of 1 mm at a 40N load are shown in **Fig. 7**. The contact trace is observed to be rough over the whole area, and the outline of the contact area can be observed clearly. The typical results of the relationship between contact load and contact area for tin or non-plated samples are shown in **Fig. 8**. The results of 5 µm tin plating samples have a larger contact area than non-plated samples due to the effect of the plated layer.
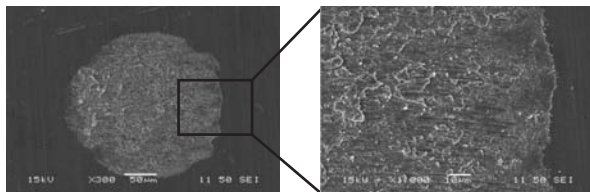
4. Force-Contact Area Relation

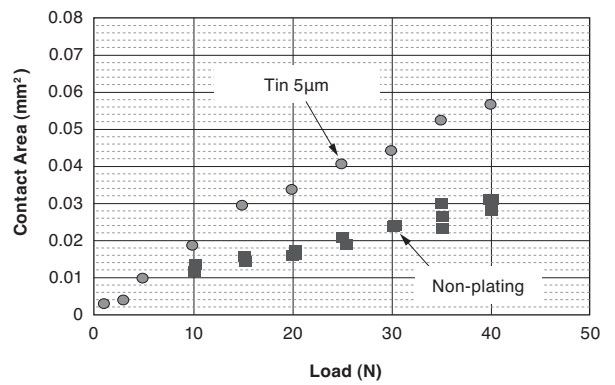Considering about embossment-flat contact, elastic deformation and plastic deformation should be investigated at first. Hertz described the contact area S in case of sphere-plane contact as **Equation (5)**.

$$S = \pi \left(\frac{2FR}{2} \left(\frac{1-\nu^2}{E} \right) \right)^{\frac{2}{3}} \quad \cdots\cdots\cdots\cdots\cdots\cdots\cdots\cdots\cdots (5)$$

Where E is Young modulus of material, R is radius of embossment, F is contact force, ν is Poisson ratio. Meanwhile, contact area in case of plastic deformation is described as **Equation (6)**.

$$S = \frac{F}{Hv} \quad \cdots\cdots\cdots\cdots\cdots\cdots\cdots\cdots\cdots\cdots\cdots (6)$$

Where Hv is Vickers hardness. **Figure 9** shows the relation between contact area and contact force in case of non-plating samples. The calculation results of **Equation (5)** and **(6)** are also shown in **Fig. 9**.

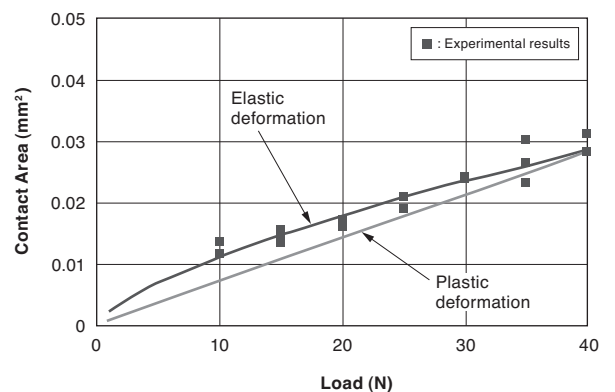**Fig. 7.** Photograph of contact area by SEM imaging

Fig. 9. Relation contact area and contact force of non-plating copper alloy

The experimental results are in good agreement with the results of elastic deformation. Thus when the sample is non-plating, the mechanism of contact area depending

on contact force is dominated by elastic deformation. When plating layer exists on the surface, the experimental results are different from the results of elastic deformation[10]. Thus, the elastic-plastic FEM contact analysis is performed. The 2-dimentonal symmetry analysis model with a plating layer is shown in **Fig. 10**. The properties of materials which are used by FEM analysis are shown in **Table 2**[11]. It is well known that the mechanical properties of bulk material and a plated layer are different due to the impurity concentration, grain size, residual stress of the plating process, etc. Meanwhile the strain-stress curve of a plated layer cannot be obtained by a tensile test experimentally; the yield stress was obtained from Vickers hardness Hv of a tin plated layer[11] as 24. The yield stress σ_y of a tin plated layer is calculated from **Equation (7)**[12].

$$Hv = 2.9\sigma_y \quad \cdots\cdots\cdots\cdots\cdots\cdots\cdots\cdots\cdots\cdots\cdots\cdots \quad (7)$$
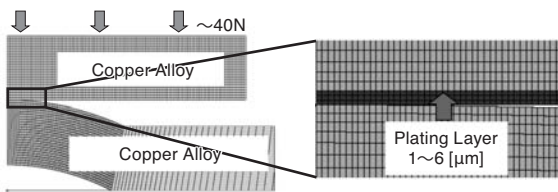

Fig. 10. 2D Axis-symmetric model with plating layer

Table 2. Material Properties

	Young Modulus (GPa)	Poisson Ratio	Yield Stress (MPa)
Copper alloy	126	0.34	485
Tin plating	46	0.34	81
Silver plating	75	0.34	21

In the case of a silver plated layer which has high ductility, the yield stress is obtained from the Hirano's formula[11] in **Equation (8)**.

$$Hv = X\sigma_y + Y \quad \cdots\cdots\cdots\cdots\cdots\cdots\cdots\cdots\cdots\cdots \quad (8)$$
$$X = 2.701, \; Y = 123 - 1.81 \times 10^{-4}A^2$$
$$+ (4.499n^2 - 5.88n + 2.525)A$$

Where A is the work hardening coefficient. Applying A = 369.7 MPa, n = 0.8 and Hv = 41 to **Equation (8)**, the yield stress of silver plating layer is obtained as 21 MPa.

Figure 11, 12 shows the comparison the experimental results with FEM results. **Figure 11** shows the tin plating layer existed on the surface. The calculation results of the hardness of bulk tin Hv 6 is also shown in **Fig. 11** just for reference. When the physical property of bulk tin was used in FEM analysis, the calculated contact area was larger than experimental results. And the FEM analysis results, which was performed on the basis of physical property values obtained from hardness of plating layer,

is a good agreement between the experimental results. Therefore, the hardness of tin plating layer influenced much on the contact area. The experimental results as well as from the FEM analysis results of silver plating are compared in **Fig. 12**. Again, a good agreement between experimental and analysis results in silver plating has been achieved.

As a result, it has become possible to predict the contact area in plated samples by modifying the stress-strain curve rather than dealing with hardness. And the mechanism of contact is elastic-plastic deformation which consists of elastic deformation of copper alloy and plastic deformation of plating layer.
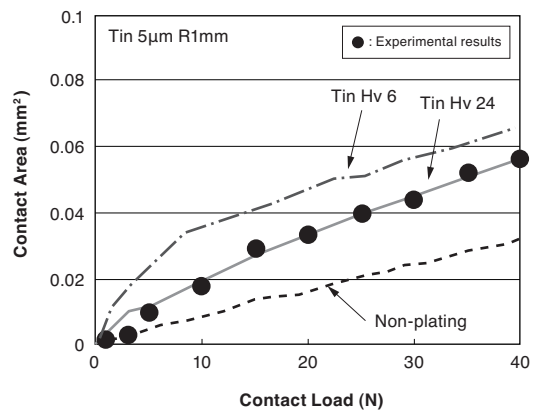

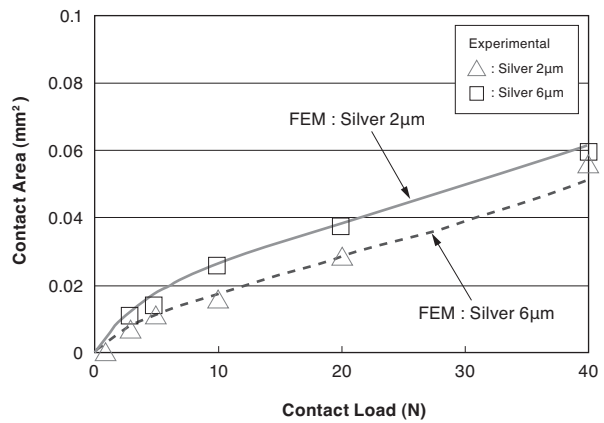**Fig. 11.** FEM results against experimental results for tin plating

Fig. 12. FEM results against experimental results for silver plating

5. Contact Area-Contact Resistance Relation

The experimental results of relation between contact area and contact resistance in various cases are shown in **Fig. 13**. X-axis shows the contact area and Y-axis shows the contact resistance. Each dot shows the results of 1 μm and 5 μm tin plating, non-plating, and 2 μm and 6 μm silver plating samples. The solid line shows the constriction resistance from **Equation (4)**.
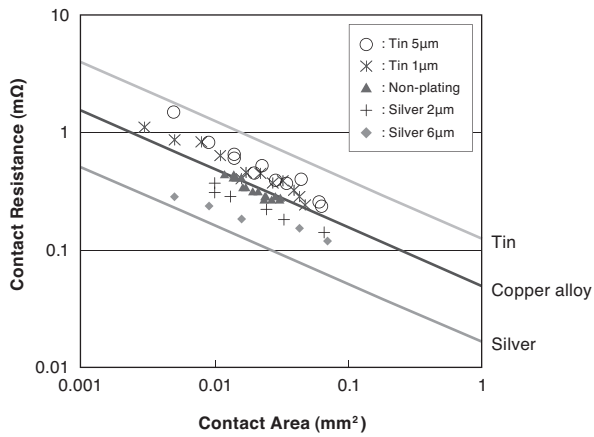
Fig. 13. Contact resistance of various samples

The contact resistance is lower when contact area is larger. The contact resistance of silver plating which has higher conductivity is lower than non-plating results. Contrariwise, the contact resistance of tin plating which has lower conductivity is higher than non-plating results. As a result, the contact resistance is changed with a plating material and thickness of contact point.

The mathematical solution of constriction resistance with a plated layer has already been solved by Tanii et al.[13]. The results show in **Equation (9)**. The constriction resistance with a plated layer is given as the constriction resistance with non-plating multiplied by the surface resistance coefficient Φ. The surface resistance coefficient is the function of four parameters: conductivity of the plating and the base metal, plating thickness d and contact radius a.

$$R_k = \Phi \frac{\rho_1}{2a} \qquad \cdots\cdots\cdots\cdots\cdots\cdots\cdots\cdots\cdots \text{(9)}$$

$$\Phi = \frac{(1-K)}{(1+K)} \cdot \frac{1}{1+\sum_{n=1}^{\infty} 2(-1)^n K^n F(2nd)} \qquad \cdots\cdots\cdots\cdots \text{(10)}$$

$$K = \frac{\sigma_2 - \sigma_1}{\sigma_2 + \sigma_1} \qquad \cdots\cdots\cdots\cdots\cdots\cdots\cdots\cdots \text{(11)}$$

$$F(x) = \int_0^{\infty} e^{-\lambda x} J_1(\lambda a) \sin(\lambda a)/\lambda \cdot d\lambda \qquad \cdots\cdots\cdots\cdots\cdots \text{(12)}$$

where J_1 is 1st-order Bessel functions, σ_1 is the conductivity of the base metal and σ_2 is the conductivity of the plating layer. **Figure 14** shows the relationship between Φ with d/a in the case of various Ks which is the ratio of conductivity of base metal and plating layer. The K of silver plating is 0.504, and the K of tin plating is -0.445 in this study. And the range of d/a in this study is from 0.01 to 0.2.

In order to understand the **Equation (9)** further, the electrical field analysis based on the Laplace equation is performed in case that a plating layer exists at contact interface. **Figure 15** shows the image of equipotential line and constriction current at contact point[12]. The equipotential line is an oval around the point of contact. **Figure 16 (a),(b)** shows the equipotential lines and current flow when a plating layer exists at a contact point. When the lower conduc-

tivity plating layer exists on the contact point, the current line is bended to outer of the contact point at plating layer interface. When the higher conductivity plating layer exists on the contact point, the current line is bended to the center of the contact point at plating layer interface.
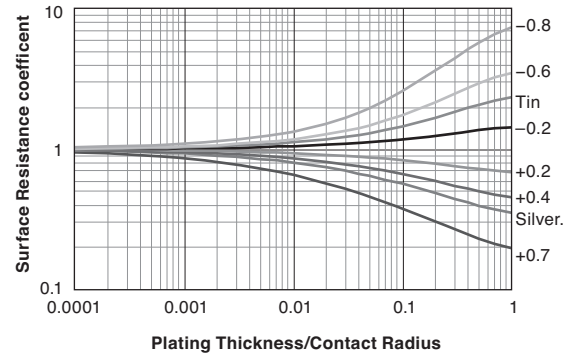

Fig. 14. Relation between surface resistance coefficient and ratio beteween plating thickness and contact radius d/a
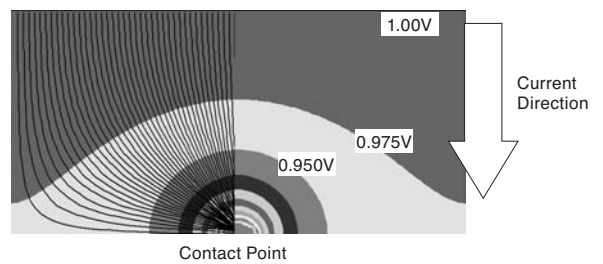

Fig. 15. Equipotential lines and current flow of a cylindrical model without plating
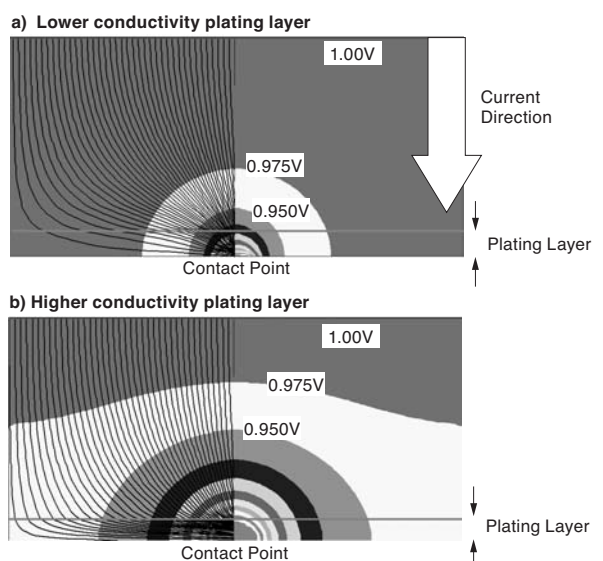

Fig. 16. Equipotential lines and current flow of a cylindrical model with plating

The relationship between theoretical contact resistances and experimental results is shown in **Fig. 17**. In the case of silver plating, which has no oxide film, the experimental results are in good agreement with the theoretical results. However, in the case of tin plating, which has oxide film, the experimental results are approximately in agreement with the theoretical results.
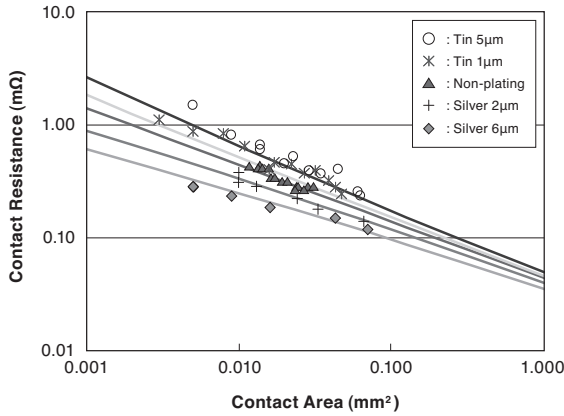

Fig. 17. Comparing contact resistance of experimental results with theoretical result

6. Prediction of Contact Resistance

The relation between contact force and contact area is obtained by **Fig. 11** and **12**. And the relation between contact area and contact resistance is obtained by **Fig. 17**. By combining these relations, the relation between contact force and contact resistance is obtained.

The contact resistance prediction and experimental results of non-plating are shown in **Fig. 18**, silver plating with a thickness of 2 μm and 6 μm in **Fig. 19** and tin plating in **Fig. 20** respectively. The solid line is a prediction line and each dot shows the experimental results. The experimental results of non-plating samples which are reduced just before resistance measurement and silver
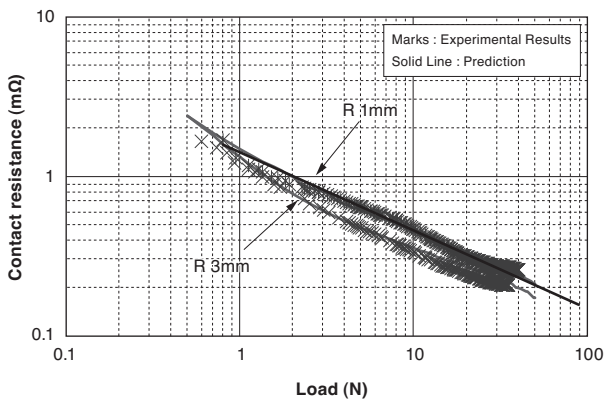

Fig. 18. Comparison of experimental results of contact resistance with theoretical results in the case of non-plating
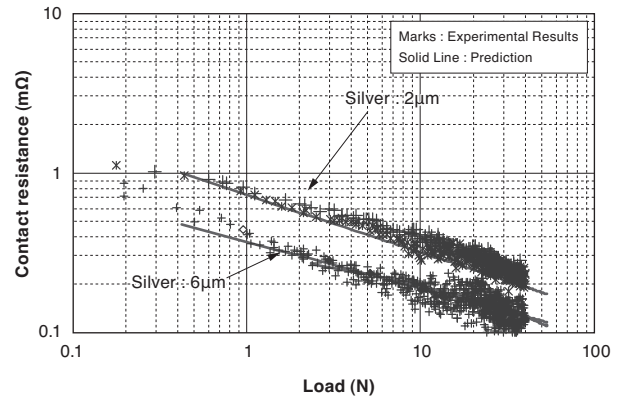

Fig. 19. Comparison of experimental results of contact resistance with theoretical results in the case of silver plating

a) Tin plating thickness: 1 μm

b) Tin plating thickness: 3 μm
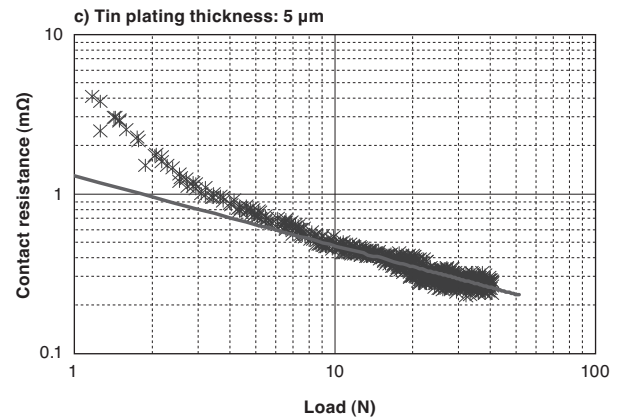

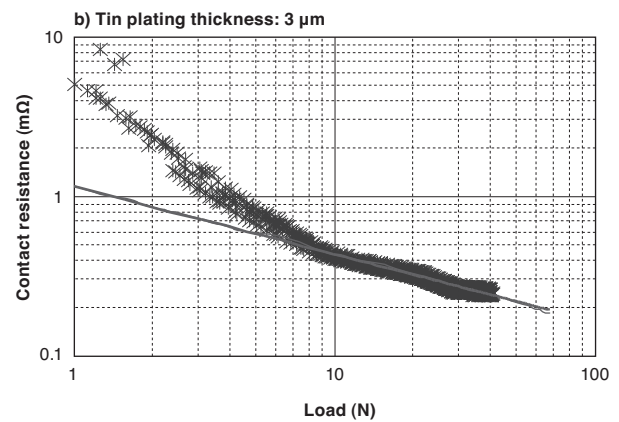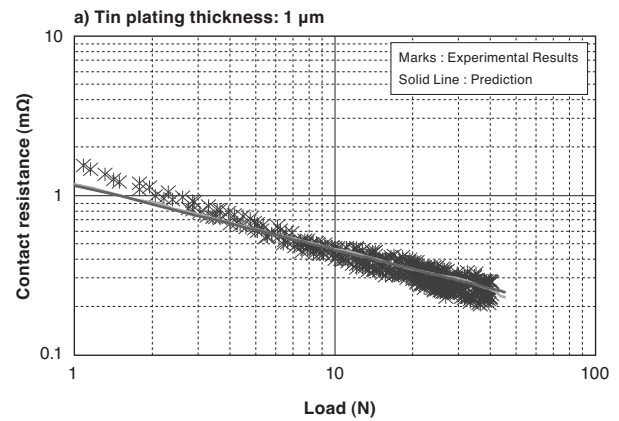**c) Tin plating thickness: 5 μm**

Fig. 20. Comparison of experimental results of contact resistance with theoretical results in the case of tin plating

plating samples which have no-oxide film are in good agreement with the calculated results. The experimental results of tin plating samples are in good agreement with experimental results in the higher load region, where contact resistance is dominated by constriction resistance. In lower load region, the contact resistance of experimental results is higher than the calculated results due to the effect of tin oxide film.

In this study, the apparent contact area has many A-spots because many adhesion marks are observed in indentation contact area (see **Fig.7**). Therefore, we find that the apparent contact area can be considered effectively equivalent to the real contact area when calculating the constriction resistance at these higher loads. For these reasons, the prediction results by FEM contact analysis are in agreement with experimental results in practical usage.

7. Conclusions

The following results are acquired from the analysis of the relationships between force and contact resistance in the cases of tin plating and silver plating.
1. The behavior of the apparent contact area with a plating layer is performed as elastic-plastic deformation which is calculated by the FEM analysis.
2. The behavior of constriction resistance with a plating layer is calculated with the constriction resistance equation in which plating layers are considered.
3. Contact resistance at each load can be predicted by combining 1. with 2.
4. In the silver-plated contact points without oxide films, the experimental results well agree with the predicted results. In the tin-plated contact points with oxide films, the predicted results agree with the measured values in a high-load region in which contact resistance is dominant by constriction resistance.
5. When the contact load is high enough and the contact spot is much about in the apparent contact area, the constriction resistance of the apparent contact area obtained by FEM contact analysis is assumed as that of the real contact area of electric contact in practical usage.

References

(1) F. Ossart, S. Noel, D. Alamarguy, S. Correia and P. Gendre, "Electro-mechanical modeling of multilayer contacts in electrical connectors," Proc. IEEE Holm Conf. Electro Contacts 53th, pp.1-8, 2007

(2) J. L. Queffelec, N. Ben Jemaa, D. Travers and G. Pethieu, "MATERIALS AND CONTACT SHAPE STUDIES FOR AUTOMOBILE CONNECTOR DEVELOPMENT," Proc. IEEE Holm Conf Electr Contacts 36th, pp.225-231, 1990

(3) M. Tukamoto, K. Sano and H. Fujimaki, "Experimental Consideration for the Contact Resistance Mechanism," Yazaki technical report, Vol.20, pp.76-79, 1996

(4) X. Hernot, A. Senouci, A. El Manfalouti and N. Ben Jema, "Contact Resistance law for elasto-plastic domains in the force range (1mN-10N)," IEICE Technical Report, EMD2002-57, pp. 10-13, 2002

(5) R. Holm, "Electric Contacts theory and application," Springer-Verlag New York Inc. (1967)

(6) Y. Saitoh, K. Iida, S. Sawada, K. Shimizu and Hattori, "Dependency of Contact Resistance on Load," Proc. of IEEE Holm conf., pp.70-75, 2007

(7) R. Holm, "Constriction resistance of an assembly of elongated a-spots," Proc. of ICEC, p.16, May 1970

(8) J. A. Greenwood, "Constriction resistance and real area of contact," Brit. J. Appl. Phys., Vol.17, pp.162-1632, 1966

(9) S. Sawada, K. Shimizu, Y. Hattori, Y. Saito, T. Tamai and K. Iida, "The effect of plating and contact shape of contact resistance in electric contact," Proc. International Conference of Electrical Contacts 24th, pp.257-261, 2008

(10) K. Shimizu, S. Shimada, S. Sawada and Y. Hattori, "Prediction of resistance of electrical contact with plated layer (2) – Contact area by FEM analysis –." IEICE Technical Report, EMD2008-89, pp.97-100, 2008-11

(11) K. Shimizu, S. Shimada, S. Sawada and Y. Hattori, "Contact area analysis by FEM with plating layer for electrical contact," IEICE Trans. Electron. Vol.E92-C, no.8, pp.1013-1019, Aug. 2009

(12) D. Tabor, The Hardness of Metals, Oxford (1951, 2000 republish)

(13) A. Hirano, M. Sakane and N. Hamada, "The effect of inelastic material constants on Vickers hardness," Proc. 2004 Annual Meeting of JSME/MMD, Vol.2004, pp.583-584, 2004

(14) T. Tanii, "The Contact points for Talking Path of the small size crossbar switch," NTT Vol.15, No.5 pp.760-791, 1966

(15) S. Sawada, K. Shimizu, Y. Hattori and T. Tamai, "Prediction of resistance of electrical contact with plated layer (1) – Theoretical analysis –." IEICE Technical Report, EMD2008-88, pp.93-96, 2008-11

Contributors (The lead author is indicated by an asterisk (*)).

S. SAWADA*
• Senior Manager, Basic Technology R&D Division, Circuits and Connection R&D Department, AutoNetWorks Technologies, Ltd.
He is engaged in the research and development of electrical connection technologies for the area of automobile wire harness at Vehicle Network Technology Laboratory in Mie University.

K. SHIMIZU
• Basic Technology R&D Department, Circuits and Connection R&D Division, AutoNetWorks Technologies, Ltd.

S. SHIMADA
• Assistant Manager, Analysis Technology Research Center

Y. HATTORI
• Senior Manager, Basic Technology R&D Division, Circuits and Connection R&D Department, AutoNetWorks Technologies, Ltd.